LAWRENCE
LIVERMORE
NATIONAL
LABORATORY

LLNL-JRNL-605214

Ultrafast Shock Initiation of Exothermic Chemistry in Hydrogen Peroxide

M. R. Armstrong, J. M. Zaug, N. Goldman, J. C. Crowhurst, W. M. Howard, J. A. Carter, M. Kashgarian, J. M. Chesser, T. W. Barbee, S. Bastea

November 29, 2012

Journal of Physical Chemistry A

Disclaimer

Control of reactivity via ultrafast compression rates

Michael R. Armstrong*, Joseph M. Zaug†, Nir Goldman, I-Feng W. Kuo, Jonathan C. Crowhurst, W. Michael Howard, Jeffrey A. Carter, Michaele Kashgarian, John M. Chesser, Troy W. Barbee, and Sorin Bastea

Physical and Life Sciences Directorate, Lawrence Livermore National Laboratory, Livermore, California 94550, USA

*email: armstrong30@llnl.gov
†equal contributor to first author, email: zaug1@llnl.gov

Abstract

We present observations of strain-rate dependent chemical reactivity of a liquid explosive, hydrogen peroxide, after laser-driven compression. Altering the laser drive energy allows us to probe both unreacted and reacted states of matter under similar thermodynamic conditions. This suggests a new, strain rate dependent mechanism for initiation of liquids under dynamic compression, rather than a conventional ‘quasiequilibrium’ kinetic mechanism. Controlled variation of the compression strain rate may lead to systematic materials synthesis of products on picosecond and nanometer scales.

Although strong compression waves have been used to study the equilibrium high pressure and temperature properties of materials for more than half a century[1–6], the study of ultrafast strain rate dependent material transformations, while promising[7], is only beginning to be fully explored. Compression waves provide an additional degree of freedom, the strain rate, for the control of reactivity with far more spatial and temporal selectivity than homogeneous, quasi-static thermodynamic parameters such as temperature and pressure. For instance, shock waves can change the thermodynamic state of a material over a picosecond time scale[1], i.e. faster than the time scale of quasi-equilibrium reaction kinetics for many reactive systems. This fundamental property of shock compression suggests the possibility of selecting reaction paths via modulation of applied compression waves on a time scale that is faster than the time scale of reaction kinetics. Strain rate dependent reactivity has implications as far reaching as high energy density materials[8,9], nanomaterials[10], chemistry under extreme conditions[1,11], new synthesis routes[12,13], highly localized chemical reactions for target-specific biological treatment[14], pressure induced phase transitions[7], and possibly the origin of life[15]. The ability to control reactivity with strain rate, including quenching[6], enables the nanoscale engineering of materials using a versatile non-equilibrium mechanism.

Shock wave initiated chemistry is an essential condition for the detonation of chemical explosives[16,17] (where energy release leads to self-sustained supersonic wave propagation), and, due to the fast time scales intrinsic to shock compression, has great potential for exploring non-equilibrium synthesis[12,13]. However, the physical and chemical

processes which occur under shock conditions are still not fully understood on either the atomic or the continuum scale[3,18–20]. Standard kinetic models of detonation do not take into account, for example, non-equilibrium effects such as strain rate effects. These models assume that chemical reactions are spontaneously initiated solely due to local thermodynamic conditions[21]. Here we present experiments which demonstrate that the applied strain rate can be used alongside the pressure and temperature to control reactivity in bulk matter, thus possibly enabling the exploration of otherwise inaccessible chemical reaction paths[15]. We show that strain rate plays a previously unrecognized role in reactivity in a liquid that undergoes an exothermic reaction, hydrogen peroxide.

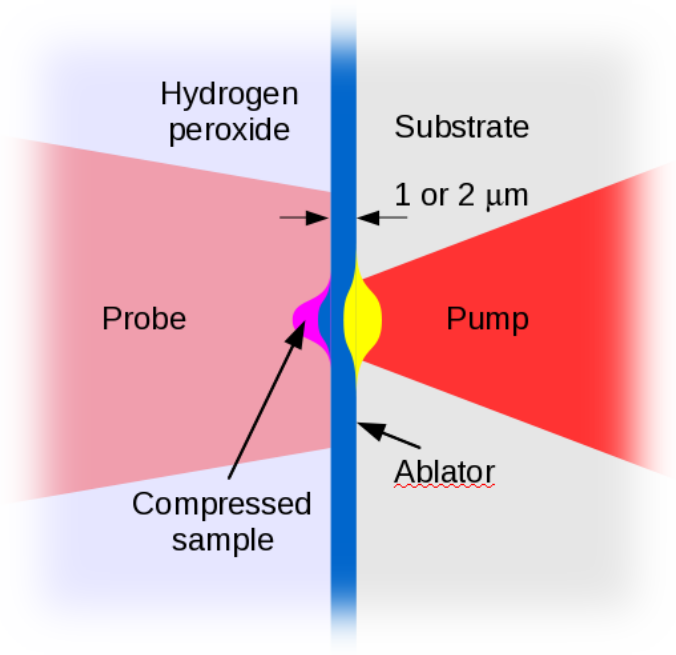

Figure 1: Scheme for shock loading and probing H_2O_2. The pump ablates a metal layer on a glass substrate, driving a shock wave into the hydrogen peroxide sample (starting from ambient pressure and temperature). The sample is compressed and heated by the moving shock wave front. The probe pulses illuminate the shocked region and the region of unshocked sample surrounding the shocked region.

Hydrogen peroxide (H_2O_2) is a model reactive system under shock loading where mixtures with and without water are known to detonate[22]. In the present work we study the behavior of H_2O_2 on picosecond time-scales using ultrafast shock wave characterization techniques[5,23–26]. Some studies have indicated microsecond timescales for its reactivity under shock compression[17], in sharp contrast to the picosecond timescales observed in simulations for similar hydrides (e.g., H_2O[19,27]). Molecular dynamics simulations have predicted that shock induced chemistry can occur in explosives over 10-100 ps[18,28], but this prediction has not yet been confirmed by characterization of the compressed thermodynamic state.

Schematics of the experiment are shown in Fig. 1. The method for generating shock compression and characterizing the shocked state of the material has been described in detail elsewhere[5,23] (more detail is given in the Supplemental Information). Essentially, the method yields the thermodynamic state of the shocked sample via measurements of shock wave speeds, analogous to longer time scale shock wave experiments, but here we obtain ultrafast time resolution. We obtain time domain data over a ~250 ps window, with a time resolution of ~10 ps. A parameterized fit to the raw data gives the piston speed (i.e. the speed at which the ablated material is compressing the H_2O_2 sample) and the resulting shock wave speed. The pressure and density of the shocked state are then calculated via the Rankine-Hugoniot jump conditions[29].

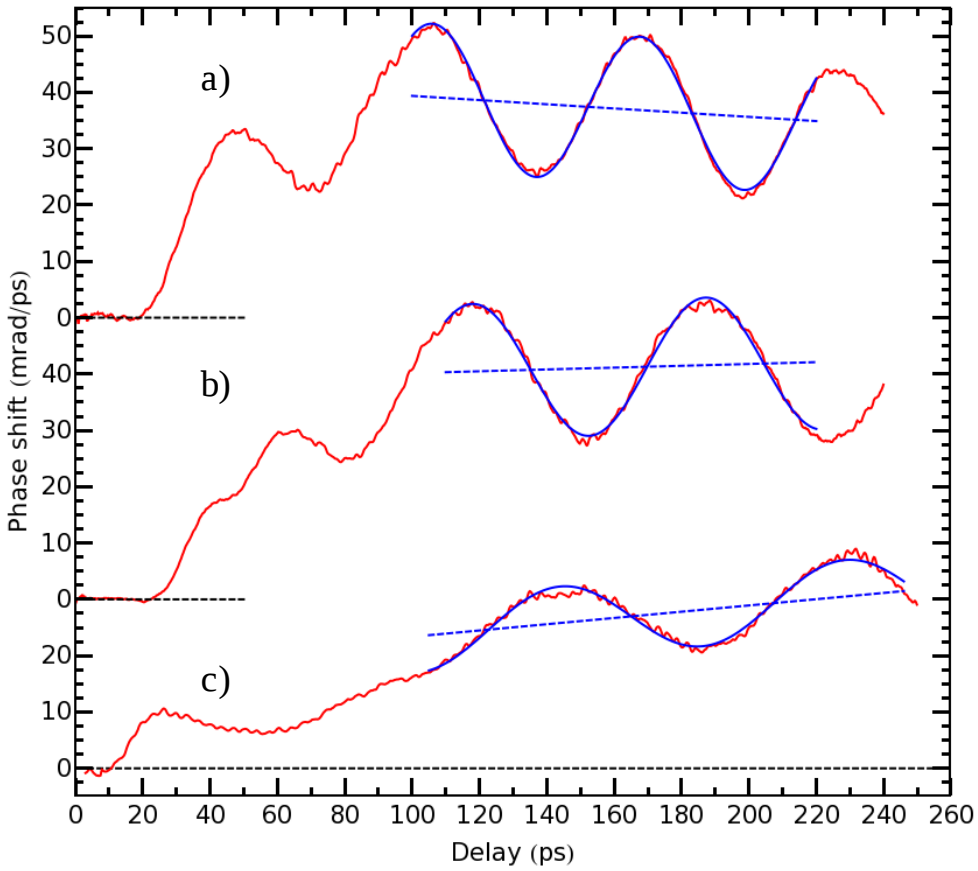

Figure 2: Examples of typical raw datasets, one from each cluster of data at the three different pump intensity/ablator thickness combinations, plotted along with fits. Black, dashed lines show the baseline for vertically offset datasets. Each dataset is a from a single shot, where the fit gives a particle and shock speed. Each cluster of speed data (shown in Fig. 3) comprises 50 such datasets. The data is shown in red, the fit is shown in blue, and the linear offset part of the fit is shown as a blue dashed line. Each fit is shown over the fitting window that was used, and the same fitting window was used for all data sets in a given cluster of data; a) high intensity, 1 μm ablator; b) low intensity, 1 μm ablator; c) low intensity, 2 μm ablator.

Typical examples of the raw phase shift data are shown in Fig. 2, along with fits to the data which give shock parameters[23]. Fifty shots each were taken at three different pump energy/ablator thickness combinations. All data were taken on a 90/10 (by weight) mixture of hydrogen peroxide and water. Each shot gives a dataset similar to one of the three shown in Fig. 2. Raw data from each shot were analyzed independently, giving an

estimate of the piston speed and the shock wave speed for every shot. A compilation of the data in piston speed/shock speed space is shown in Fig. 3. Each cluster of points corresponds to a different pump intensity, where the peak intensity used was ~10^{11} W/cm^2 (see the Supplemental Information).

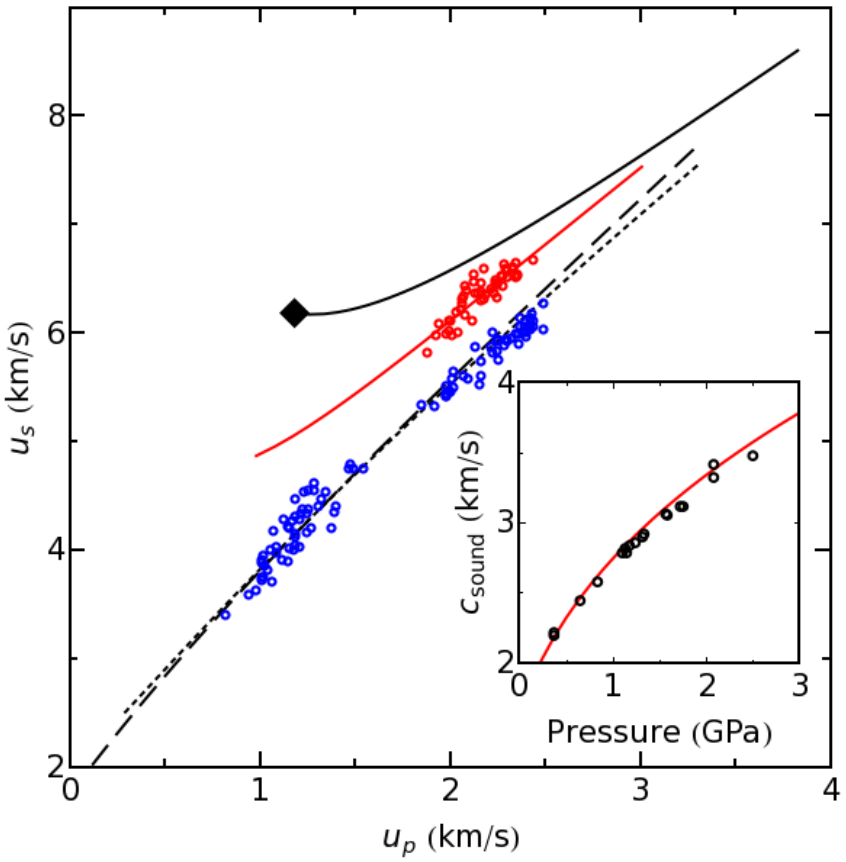

Figure 3: Piston and shock wave speeds for three different combinations of pump energy and ablator thickness. Points are shown along a partially reacted Hugoniot (red points) and an unreacted Hugoniot (blue points). Also shown are thermochemical calculations[35] for the 50% reacted Hugoniot (solid red line), unreacted Hugoniot derived from measured sound speeds (black, dashed line), and the "universal" liquid Hugoniot[33] for H_2O_2 (black, dotted line). The solid black line is a thermochemical calculation of the fully reacted Hugoniot and the black diamond specifies the steady state detonation condition. Sound speeds (black open circles) in unreacted H_2O_2 at room temperature and high pressures, measured using impulsively stimulated light scattering (ISLS)[43] in a diamond anvil cell are shown in the inset. The sample is solid at room temperature above approximately 2 GPa. The red line in the inset is a fit based on an exp6-polar model for liquid H_2O_2, similar with the one developed for water[30]. This model predicts the Hugoniot shown as a dashed black line in the main figure.

Due to the acoustic transit delay between the ablator/sample interface and the shock front, an independent change in the piston speed does not immediately result in a corresponding change in the shock speed. Errors due to this effect were found to be similar to the scatter of the data, less than 1.7% and 3.6% for the higher and lower particle speed data sets, respectively (see the Supplemental Information).

The two (blue) clusters of lower intensity shots match very well the shock Hugoniot (thermodynamic end states) of 90% hydrogen peroxide in the absence of chemical reactions, henceforth designated as unreacted Hugoniot (shown in Fig. 3 by a dotted line), calculated using an *exp6-polar* model[30] for hydrogen peroxide, derived from measured sound speeds (see Fig. 3, inset) at high pressures (and further constrained by critical point[31] and dipole moment data[32]), as well as the "universal" liquid Hugoniot[33] for unreacted 90% hydrogen peroxide (shown in the figure by a dashed line).

In contrast, the higher intensity shots (red points in Fig. 3) exhibit larger shock wave speeds for a given piston speed, consistent with shock induced chemistry occurring over the duration of the experiment. In particular, exothermic chemistry results in an increase in volume in the shock compressed sample due to the expanding hot, gaseous products (i.e. H_2O and O_2). This produces a higher shock wave speed than would be obtained if the material did not react. The higher intensity data agree very well with the partially (50%) reacted Hugoniot (in red) given by thermochemical calculations[34] based on *exp6-polar* modeling of the fluid mixture. Also shown in Fig. 3 are similar calculations for the fully

reacted Hugoniot (black line) and the steady state detonation speed (black diamond); the latter matches very well available experimental results[35]. It is also worth noting that each of the higher intensity shots produced a bubble of gas in the shocked region, whereas nominally unreacted shots did not. Although neither the composition of these bubbles nor the time scale of their formation could be determined, it is very likely that they formed as a result of the decomposition of hydrogen peroxide into water and gaseous molecular oxygen.

Molecular dynamics (MD) simulations provide an independent route to equation of state data and also elucidate changes in phase or chemical speciation that occur during dynamic compression. Simulating the breaking and forming of chemical bonds behind a shock front frequently requires the use of a quantum theory[15]. The density functional tight binding method (DFTB) holds promise as a semi-empirical quantum approach for simulations of materials at high pressures and temperatures. DFTB (with self-consistent atomic charges) is an approximate quantum simulation technique that allows for several orders of magnitude increase in computational efficiency while retaining most of the accuracy of standard quantum simulations, (e.g., Kohn-Sham Density Functional Theory[36]). DFTB allows for longer time and length scales to be achieved than with DFT while still providing a description of the electronic states. We observe excellent agreement between DFTB and DFT for the H_2O_2 pressure-volume relation at 0 K up to ~50 GPa (See Supplementary Information). DFTB has been shown to provide accurate descriptions of chemical reactivity for number of systems under extreme conditions,

including nitromethane[18] and HMX[37].

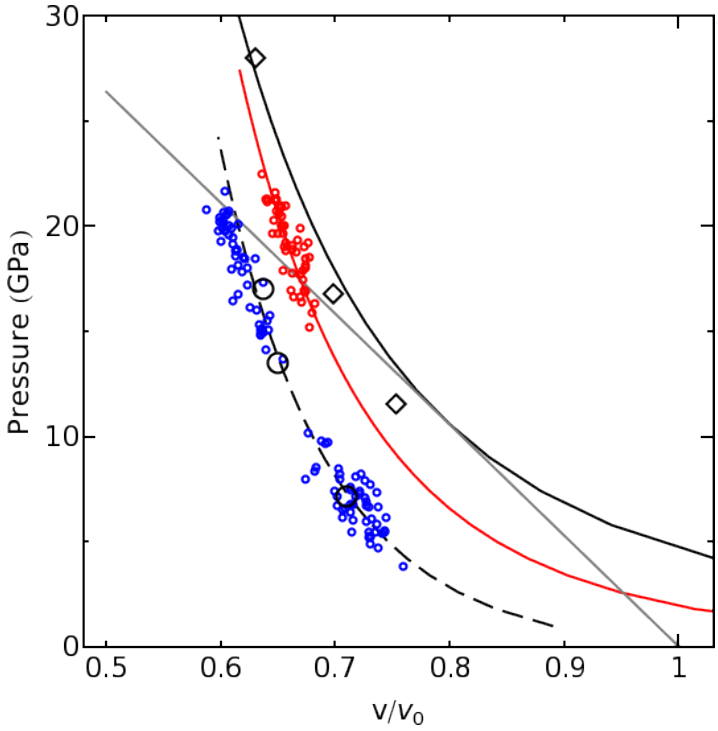

Figure 4: Thermodynamic states given by the measured particle and shock wave speeds of Fig. 3; specific volumes are normalized by the initial values. The style of lines and points are consistent with Fig. 3. The open black symbols are results calculated using DFTB molecular dynamics simulations for pure H_2O_2; diamonds correspond to the reacted Hugoniot, and circles correspond to the unreacted Hugoniot. The Rayleigh line for 90% H_2O_2 (detonation velocity 6.18 km/s) is shown in gray; it is tangent to the reacted Hugoniot at the Chapman-Jouguet point and it intersects the unreacted Hugoniot at the von Neumann spike[16].

In order to perform simulations of the unique thermodynamic conditions of a shock[18], we use the Multi-scale Shock compression Simulation Technique (MSST)[38] MSST is a simulation methodology based on MD and the Navier-Stokes equations for compressible flow. Instead of simulating a planar shock wave within a large computational cell with many atoms, the MSST computational cell follows a Lagrangian point through the shock

wave. MSST does not include non-planar shock waveforms. MSST has been shown to accurately reproduce the shock Hugoniot (thermodynamic end states) of a number of systems[15,18,27] as well as the sequence of thermodynamic states throughout the reaction zone of shock compressed explosives, and the same shock wave profiles, physics, and chemistry found in direct, multi-million particle simulation of shock compression (see Supplemental Information for more details).

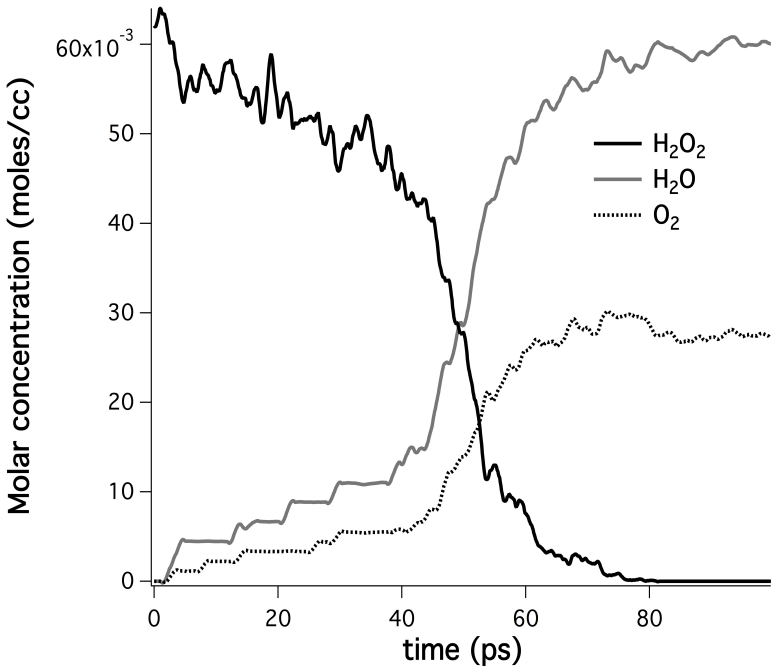

Figure 5: Mole concentrations of reactants and products from DFTB simulations of detonation in hydrogen peroxide along the thermodynamic trajectory of the steady detonation wave, where time is measured from the arrival of the lead shock in a given parcel of unreacted material.

Figure 4 shows the Hugoniot end-states of Fig 3 in pressure-volume space, along with DFTB-MD simulation results for pure H_2O_2. Results from the DFTB simulations are in agreement with experimental data for both unreacted and reacted Hugoniot curves. The

occurrence of chemistry, i.e. H_2O_2 dissociation, and the extent of the chemical reaction were directly identified in the simulations by analyzing the molecular species population as a function of time. The MD results show a transition from unreactive to reactive shocks as the shock velocity is increased (see Fig. 4), with chemical reactions occurring on time scales of roughly 100 ps (see Fig. 5). The product species found for the reactive shocks were primarily H_2O and O_2, with negligible amounts of other molecules. We note that although in the experiments the nominally reacted shots do not appear to reach steady state hydrodynamic conditions (consistent with a detonation wave), they are clearly consistent with chemical reactions occurring on time scales comparable to the simulation results. Future modeling of the entire experimental set-up using hydrodynamics/reaction coupling at the continuum scale may enable the direct determination of chemical reaction rates from the experimental results.

We note that the measured particle speeds of one unreacted cluster of shots (at 2 km/s particle speed) are larger than the particle speed corresponding to the steady state detonation (the black diamond in Fig. 3 and Refs. 17 and 35). This likely indicates that shock induced reactions in this system are kinetically limited on the time scale of the present experiment. Previous experimental results on hydrogen peroxide have shown that just above the detonation threshold (13.3 GPa[17]) the formation of a detonation wave occurs at least ~1 μs[17] subsequent to shock compression, far longer than the time scale of the present work. We find that the high intensity data is consistent with a partially reacted Hugoniot (see Fig. 4), indicating that the compression wave does not evolve to a steady-state detonation over the duration of the experimental window.

Longer time scale experiments at shock pressures just above the detonation threshold have observed propagation of a shock front well into the sample without reaction, followed, after an incubation time, by the initiation of reactions at the piston, and the propagation of a "superdetonation" reaction front from the piston to the shock front[39]. In the present work, observation of reactions within 100 ps of shock arrival in the sample indicates promp reaction behind the shock front, with a time scale for complete reaction comparable to the ~100 ps time scales observed in our MD simulations (see Fig. 5). Further, we note lower pressures in some reacted data than in unreacted data (both at ~2 km/s piston speed). This is indicative of an ultrafast initiation of decomposition chemistry that is dependent on the strain rate applied to the sample and is initiated at the shock front itself, contrary to previous work. This type of ultrafast strain rate dependent phenomena,

which is analogous to strain rate dependent plasticity observed in the deformation of metals[5,40,41], is observed here in a shock compressed liquid for the first time. Our results suggest that non-equilibrium effects due to shock strain rate could be more important for the detonation of liquids than previously thought. We note in particular that we observed unreacted states up to the von Neumann pressure[16,42] for a steady detonation. This suggests that reactions in H_2O_2 may be initiated by a strain rate mechanism even in a steady state detonation wave.

These remarkable features suggest the existence of an strain rate threshold for the initiation of chemical reactions on sub-nanosecond timescales – a reaction mechanism that is fundamentally different than quasi-equilibrium kinetics, which are generally assumed in models of chemical reactions (where initiation of chemical reactivity is assumed to occur virtually instantaneously under a given set of thermodynamic conditions). The study of shock initiation thresholds in exothermic liquids[17,39] has long suggested that the observation of chemical reactions in these systems requires incubation times of order microseconds, where homogenous nucleation-like initiation of chemical reactions occurs in the compressed material behind the initial unreactive shock. The results summarized here indicate that ultrafast drives can be used to control chemical reactivity on much shorter time scales, consistent with those of the MD simulations. We speculate that this behavior is due to the extremely high strain rates that are typical of shocks[23], which, at sufficiently high shock wave strength, lead to prompt initiation of chemical reactions before an unreactive shock wave has time to develop. Ultrafast

experimental techniques may thus be useful for controlling chemical reaction rates via a non-equilibrium drive mechanism. Picosecond time resolution in such shock-induced chemistry experiments affords the observation and possibly the control of reactivity, via strain rate, over time scales where kinetic models do not apply, which may ultimately enable the nanoscale engineering of material synthesis.

We acknowledge useful conversations with L. E. Fried, D. Dlott, S. McGrane, W. J. Nellis, J. Forbes, and R. Manaa. This research was performed under the auspices of the U.S. Department of Energy by Lawrence Livermore National Laboratory under Contract No. DE-AC52-07NA27344, and it was funded by Laboratory Directed Research and Development grant 11ERD067 with S.B. as principal investigator.

References

1. Nellis, W. J. Dynamic compression of materials: metallization of fluid hydrogen at high pressures. *Rep. Prog. Phys.* **69**, 1479–1580 (2006).
2. Dlott, D. D. New Developments in the Physical Chemistry of Shock Compression. *Annual Review of Physical Chemistry, Vol 62* **62**, 575–597 (2011).
3. McGrane, S. D., Moore, D. S. & Funk, D. J. Shock Induced Reaction Observed via Ultrafast Infrared Absorption in Poly(vinyl nitrate) Films. *J. Phys. Chem. A* **108**, 9342–9347 (2004).
4. Patterson, J. E., Lagutchev, A., Huang, W. & Dlott, D. D. Ultrafast dynamics of shock compression of molecular monolayers. *Phys. Rev. Lett.* **94**, 015501 (2005).
5. Crowhurst, J. C., Armstrong, M. R., Knight, K. B., Zaug, J. M. & Behymer, E. M. Invariance of the Dissipative Action at Ultrahigh Strain Rates Above the Strong Shock Threshold. *Phys. Rev. Lett.* **107**, 144302 (2011).
6. Carter, J. A., Zaug, J. M., Nelson, A. J., Armstrong, M. R. & Manaa, M. R. Ultrafast Shock Compression and Shock-Induced Decomposition of 1,3,5-Triamino-2,4,6-trinitrobenzene Subjected to a Subnanosecond-Duration Shock: An Analysis of Decomposition Products. *J. Phys. Chem. A* **116**, 4851–4859 (2012).
7. Vailionis, A. *et al.* Evidence of superdense aluminium synthesized by ultrafast microexplosion. *Nat. Commun.* **2**, 1 (2011).
8. Nellis, W. *et al.* The Nature of the Interior of Uranus Based on Studies of Planetary Ices. *Science* **240**, 779–781 (1988).
9. Ma, Y., Oganov, A. R., Li, Z., Xie, Y. & Kotakoski, J. Novel High Pressure Structures

of Polymeric Nitrogen. *Phys. Rev. Lett.* **102**, 065501 (2009).

10. Decarli, P. & Jamieson, J. Formation of Diamond by Explosive Shock. *Science* **133**, 1821 (1961).
11. Nellis, W., Holmes, N., Mitchell, A. & Vanthiel, M. Phase-Transition in Fluid Nitrogen at High-Densities and Temperatures. *Phys. Rev. Lett.* **53**, 1661–1664 (1984).
12. Mochalin, V. N., Shenderova, O., Ho, D. & Gogotsi, Y. The properties and applications of nanodiamonds. *Nat. Nanotechnol.* **7**, 11–23 (2012).
13. Qu, Y., Li, X., Wang, X. & Liu, D. Detonation synthesis of nanosized titanium dioxide powders. *Nanotechnology* **18**, 205602 (2007).
14. Jin, C. Y., Li, Z., Williams, R. S., Lee, K.-C. & Park, I. Localized Temperature and Chemical Reaction Control in Nanoscale Space by Nanowire Array. *Nano Lett.* **11**, 4818–4825 (2011).
15. Goldman, N., Reed, E. J., Fried, L. E., Kuo, I.-F. W. & Maiti, A. Synthesis of glycine-containing complexes in impacts of comets on early Earth. *Nat. Chem.* **2**, 949–954 (2010).
16. Zeldovich, I. B. *Theory of Detonation*. (Academic Press: New York and London, 1960).
17. Sheffield, S. A. *et al.* Shock Initiation and Detonation Study on High Concentration H_2O_2/H_20 Solutions Using In-Situ Magnetic Gauging. *Proceedings of the 14th International Detonation Symposium* 601–610 (2010).
18. Reed, E. J., Manaa, M. R., Fried, L. E., Glaesemann, K. R. & Joannopoulos, J. D. A transient semimetallic layer in detonating nitromethane. *Nat. Phys.* **4**, 72–76 (2008).

19. Wu, C. J., Fried, L. E., Yang, L. H., Goldman, N. & Bastea, S. Catalytic behaviour of dense hot water. *Nat. Chem.* **1**, 57–62 (2009).
20. Radulescu, M. I. & Tang, J. Nonlinear Dynamics of Self-Sustained Supersonic Reaction Waves: Fickett's Detonation Analogue. *Phys. Rev. Lett.* **107**, 164503 (2011).
21. Kirkwood, J. & Wood, W. Structure of a Steady-State Plane Detonation Wave with Finite Reaction Rate. *J. Chem. Phys.* **22**, 1915–1919 (1954).
22. Gibson, L. L., Bartram, B., Dattelbaum, D. M., Sheffield, S. A. & Stahl, D. B. A Remote Liquid Target Loading System for a Two-Stage Gas Gun. *Shock Compression of Condensed Matter - 2009, Pts 1 and 2* **1195**, 133–136 (2009).
23. Armstrong, M. R., Crowhurst, J. C., Bastea, S. & Zaug, J. M. Ultrafast observation of shocked states in a precompressed material. *J. Appl. Phys.* **108**, 023511 (2010).
24. Bolme, C. A., McGrane, S. D., Moore, D. S. & Funk, D. J. Single shot measurements of laser driven shock waves using ultrafast dynamic ellipsometry. *J. Appl. Phys.* **102**, 033513 (2007).
25. Benuzzi-Mounaix, A. *et al.* Chirped pulse reflectivity and frequency domain interferometry in laser driven shock experiments. *Phys. Rev. E* **60**, R2488–R2491 (1999).
26. Evans, R. *et al.* Time- and Space-Resolved Optical Probing of Femtosecond-Laser-Driven Shock Waves in Aluminum. *Phys. Rev. Lett.* **77**, 3359 (1996).
27. Goldman, N. *et al.* Ab initio simulation of the equation of state and kinetics of shocked water. *J. Chem. Phys.* **130**, 124517 (2009).
28. Reed, E. J., Rodriguez, A. W., Manaa, M. R., Fried, L. E. & Tarver, C. M. Ultrafast

Detonation of Hydrazoic Acid (HN_3). *Phys. Rev. Lett.* **109**, 038301 (2012).

29. Zel'dovich, B. Y. & Raizer, Y. P. *Physics of shock waves and high-temperature hydrodynamic phenomena*. (Dover Publications: Mineola, NY, 2002).
30. Bastea, S. & Fried, L. E. Exp6-polar thermodynamics of dense supercritical water. *J. Chem. Phys.* **128**, 174502 (2008).
31. Nikitin, E. D., Pavlov, P. A., Popov, A. P. & Nikitina, H. E. Critical properties of hydrogen peroxide determined from direct measurements. *The Journal of Chemical Thermodynamics* **27**, 945–952 (1995).
32. Cohen, E. A. & Pickett, H. M. The dipole moment of hydrogen peroxide. *Journal of Molecular Spectroscopy* **87**, 582–583 (1981).
33. Woolfolk, R. W., Cowperthwaite, M. & Shaw, R. A "universal' Hugoniot for liquids. *Thermochimica Acta* **5**, 409 (1973).
34. Bastea, S. & Fried, L. E. Chemical equilibrium detonation. *Shock Wave Science and Technology Reference Library* **6**, (2012).
35. Engelke, R., Sheffield, S. A. & Davis, L. L. Experimental and predicted detonation parameters for liquid-phase H_2O_2/H_20 mixtures. *J. Phys. Chem. A* **104**, 6894–6898 (2000).
36. Kohn, W. & Sham, L. Self-Consistent Equations Including Exchange and Correlation Effects. *Physical Review* **140**, 1133 (1965).
37. Manaa, M. R., Fried, L. E., Melius, C. F., Elstner, M. & Frauenheim, T. Decomposition of HMX at extreme conditions: A molecular dynamics simulation. *J. Phys. Chem. A* **106**, 9024–9029 (2002).

38. Reed, E. J., Fried, L. E. & Joannopoulos, J. D. A method for tractable dynamical studies of single and double shock compression. *Phys. Rev. Lett.* **90**, 235503 (2003).
39. Hardesty, D. R. An investigation of the shock initiation of liquid nitromethane. *Combustion and Flame* **27**, 229–251 (1976).
40. Whitley, V. H. *et al.* The elastic-plastic response of aluminum films to ultrafast laser-generated shocks. *J. Appl. Phys.* **109**, 013505 (2011).
41. Ashitkov, S. I., Agranat, M. B., Kanel', G. I., Komarov, P. S. & Fortov, V. E. Behavior of aluminum near an ultimate theoretical strength in experiments with femtosecond laser pulses. *JETP Lett.* **92**, 516–520 (2010).
42. Davis, W. The Detonation of Explosives. *Sci.Am.* **256**, 106 (1987).
43. Zaug, J., Slutsky, L. & Brown, J. Equilibrium Properties and Structural Relaxation in Methanol to 30.4 GPa. *J. Phys. Chem.* **98**, 6008–6016 (1994).